Harmful Algae 122 (2023) 102369

Contents lists available at ScienceDirect

Harmful Algae

journal homepage: www.elsevier.com/locate/hal

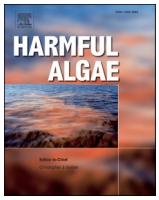

Original Article

Diversity of the holopelagic *Sargassum* microbiome from the Great Atlantic *Sargassum* Belt to coastal stranding locations

Tom Theirlynck [a,b], Inara Regina W. Mendonça [c], Aschwin H. Engelen [d], Henk Bolhuis [a], Ligia Collado-Vides [e], Brigitta I. van Tussenbroek [f], Marta García-Sánchez [f,g], Erik Zettler [a], Gerard Muyzer [b], Linda Amaral-Zettler [a,b,*]

[a] Department of Marine Microbiology and Biogeochemistry, NIOZ Royal Netherlands Institute for Sea Research, Den Burg, Texel, The Netherlands
[b] Department of Freshwater and Marine Ecology, Institute for Biodiversity and Ecosystem Dynamics, University of Amsterdam, Amsterdam 1098 XH, The Netherlands
[c] Department of Botany, Institute of Biosciences, University of São Paulo, Rua do Matão 277, São Paulo, 05508-090, Brazil
[d] Centro de Ciências do Mar, Universidade do Algarve, Gambelas, 8005-139, Faro, Portugal
[e] Department of Biological Sciences, Institute for Water and Environment, Florida International University, 11200 SW 8th Street, Miami, 33199, FL, United States of America
[f] Unidad Académica de Sistemas Arrecifales, Instituto de Ciencias del Mar y Limnología-UNAM, Prol. Av. Niños Héroes S/N, Puerto Morelos, C.P. 77580, Q. Roo, Mexico
[g] Instituto de Ingeniería, UNAM, Ciudad Universitaria, Ciudad de México, C.P. 04510, Mexico

ARTICLE INFO

Edited by Editor Name: Dr Holly Bowers

Keywords:
Bacteria
Host-specificity
Vibrio
Ecosystem health
Dysbiosis

ABSTRACT

The holopelagic brown macroalgae *Sargassum natans* and *Sargassum fluitans* form essential habitats for attached and mobile fauna which contributes to a unique biodiversity in the Atlantic Ocean. However, holopelagic *Sargassum natans* (genotype I & VIII) and *Sargassum fluitans* (genotype III) have begun forming large accumulations with subsequent strandings on the western coast of Africa, the Caribbean and northern Brazil, threatening local biodiversity of coastal ecosystems and triggering economic losses. Moreover, stranded masses of holopelagic *Sargassum* may introduce or facilitate growth of bacteria that are not normally abundant in coastal regions where *Sargassum* is washing ashore. Hitherto, it is not clear how the holopelagic *Sargassum* microbiome varies across its growing biogeographic range and what factors drive the microbial composition. We determined the microbiome associated with holopelagic *Sargassum* from the Great Atlantic *Sargassum* Belt to coastal stranding sites in Mexico and Florida. We characterized the *Sargassum* microbiome via amplicon sequencing of the 16S V4 region hypervariable region of the rRNA gene. The microbial community of holopelagic *Sargassum* was mainly composed of photo(hetero)trophs, organic matter degraders and potentially pathogenic bacteria from the *Pseudomonadaceae, Rhodobacteraceae* and *Vibrionaceae. Sargassum* genotypes *S. natans* I, *S. natans* VIII and *S. fluitans* III contained similar microbial families, but relative abundances and diversity varied. LEfSE analyses further indicated biomarker genera that were indicative of *Sargassum S. natans* I/VIII and *S. fluitans* III. The holopelagic *Sargassum* microbiome showed biogeographic patterning with high relative abundances of *Vibrio* spp., but additional work is required to determine whether that represents health risks in coastal environments. Our study informs coastal management policy, where the adverse sanitary effects of stranded *Sargassum* might impact the health of coastal ecosystems.

1. Introduction

The marine macroalgal genus *Sargassum* is one of the most species-rich genera among the brown macroalgae, encompassing over 350 recognized species (Guiry and Guiry, 2022). Most of the species are benthic and are attached via a holdfast; although some species, like *S. horneri* may form drifting masses that last for several months (Fidai et al., 2020). Only two truly holopelagic *Sargassum* species are described: *S. natans* and *S. fluitans*. Both spend their entire life cycle floating in the Atlantic Ocean and reproduce by vegetative fragmentation (Butler and Stoner, 1984; Dawes et al., 2008). In the tropical Atlantic, three *Sargassum* genotypes dominate: *S. natans* I, *S. fluitans* III

* Corresponding author at: Department of Marine Microbiology and Biological Geochemistry, NIOZ Royal Netherlands Institute for Sea Research, P.O. Box 59, Den Burg, 1790 AB The Netherlands.
E-mail address: linda.amaral-zettler@nioz.nl (L. Amaral-Zettler).

https://doi.org/10.1016/j.hal.2022.102369
Received 1 July 2022; Received in revised form 26 October 2022; Accepted 7 December 2022
Available online 30 December 2022

and the recently abundant *S. natans* VIII.

Often referred to as the "golden floating rainforest", holopelagic *Sargassum* plays a vital role in the biodiversity of the pelagic Atlantic Ocean. Since holopelagic *Sargassum* is often the only form of substrate in open waters, it serves important ecosystem functions; it supports more than 100 species of fish and invertebrates (Coston-Clements et al., 1991; Niermann, 1986), serves as a nursery for a wide array of species including endangered species such as sea turtles (Laffoley et al., 2011; Wells and Rooker, 2004) and houses 10 endemic species (Fine, 1970; Hemphill, 2005; Laffoley et al., 2011). Holopelagic *Sargassum* also plays a role in the local carbon sequestration of the Atlantic Ocean by incorporating CO_2 through photosynthesis and subsequently sinking to deeper waters (Gouvêa et al., 2020; Hu et al., 2021; Johnson and Richardson, 1977).

Since 2011, however, holopelagic *Sargassum* has started forming unprecedented accumulations in the coastal environments of the Caribbean, the United States, Brazil and Africa that threaten biodiversity (Smetacek and Zingone, 2013), local economies (Partlow and Martinez, 2015) and coastline stability (van Tussenbroek et al., 2017). As holopelagic *Sargassum* spreads to coastal regions it washes ashore and produces rotting masses, characterized by leachates and a brown water color (van Tussenbroek et al., 2017). Moreover, holopelagic *Sargassum* causes significant human health risks to local communities by accumulating large amounts of H_2S when rotting that can cause neurological, digestive and respiratory disorders (Devault et al., 2021; Resiere et al., 2020).

Several hypotheses have been suggested as possible causes for these recent accumulations, that have been referred to as the Great Atlantic *Sargassum* Belt, linked to the North Equatorial Recirculation Region (NERR) as a source region (Gower et al., 2013; Johnson et al., 2012; Wang et al., 2019). One hypothesis is that an increase in nutrients supplied by the Amazon and Congo Rivers due to combined effects of deforestation, agro-industrial and urban activities of these river areas has fed holopelagic *Sargassum* accumulations (Djakouré et al., 2017; Hu et al., 2021; Oviatt et al., 2019). Another hypothesis is that positive increases in sea surface temperatures in the NERR (Brooks et al., 2018; Djakouré et al., 2017) could stimulate holopelagic *Sargassum* growth either directly by reaching a more suitable optimal growth temperature for holopelagic *Sargassum*, or more importantly, indirectly by increasing the nutrient availability via increased rainfall associated run-off. Moreover, anomalies in the North Atlantic Oscillation (NAO) may have transported holopelagic *Sargassum* from the Sargasso Sea to the NERR, creating a seed population for the *Sargassum* blooms (Johns et al., 2020). Overall, the consensus of these studies is that the recent holopelagic *Sargassum* accumulations are a result of climate change related factors fed by additional nutrient inputs of nitrate and phosphate from surrounding rivers systems (Djakouré et al., 2017; Johns et al., 2020; Lapointe et al., 2021; Sissini et al., 2017; Wang et al., 2019).

Holopelagic *Sargassum* is not only a favored habitat for invertebrate and vertebrate fauna, but the algae function as a microbial substrate as well, promoting microbial colonization by releasing high amounts of organic matter. Research on the microbial community associated with holopelagic *Sargassum* remains scarce. Torralba et al. (2017) indicated that the holopelagic *Sargassum* microbiome features a diverse microbial community compared to the neighboring seawater, largely composed of photosynthetic and nitrogen-fixing bacteria belonging to the *Rhodobacteraceae* and *Cyanobacteria*. Hervé et al. (2021) showed that dissolved organic matter (DOM)-degrading bacteria are likely present in groups such as *Saprospiraceae* and *Flavobacteraceae*. Furthermore, holopelagic *Sargassum* genotypes were reported to host similar bacterial OTUs (Operational Taxonomic Units) (Michotey et al., 2020), which is surprising since macroinvertebrate communities may vary between *Sargassum* genotypes (Govindarajan et al., 2019; Martin et al., 2021). Variations in the holopelagic *Sargassum* microbiome are thus far largely unexplored, but *Sargassum* genotype specificity in the microbial community is hypothesized.

Michotey et al. (2020) showed that at several locations across the Great Atlantic *Sargassum* Belt (GASB), high relative abundances of *Vibrio* and *Alteromonas* are associated with the *Sargassum* microbiome, of which six *Vibrio* OTUs were identified as possible pathogens. These high *Vibrio* relative abundances were hypothesized as being linked to holopelagic *Sargassum* growth, resulting in elevated *Sargassum* exudates that are high in dissolved organic carbon predominantly in open waters rather than stations closer to the shore (Michotey et al., 2020). However, that study considered mostly open water stations rather than coastal stranding locations and there are likely structural differences in the microbiome when holopelagic *Sargassum* enters coastal waters and forms brown tides (Hervé et al., 2021; Michotey et al., 2020). As macroalgal microbiomes enter dysbiosis, relative abundances of pathogenic opportunistic bacteria may increase in contrast to the microbiome of healthy macroalgae (Minich et al., 2018). Moreover, holopelagic *Sargassum* might not only introduce its own associated bacteria, but might also serve as a substrate and carbon source for coastal pathogens that rapidly increase in abundance as *Sargassum* accumulates and decomposes on the coast, which could have large implications for coastal ecosystems.

Given all of the above it is currently unclear how the *Sargassum* microbiome, along with possible hitchhiking pathogens, varies across the GASB, and from open ocean to coastal locations where *Sargassum* strands. Here, we characterized the microbial community composition associated with *S. natans* I, *S. natans* VIII and *S. fluitans* III from the GASB to coastal stranding locations in Mexico and Florida. The holopelagic *Sargassum* microbiome was characterized using amplicon sequencing of the V4 hypervariable region of the 16S rRNA gene in 117 samples collected during 2018–2019. Our findings highlight varying biogeography and genotype-specificity of the holopelagic *Sargassum* microbiome.

2. Material and methods

2.1. Description of sampling locations and water sampling

Samples of *S. natans* I, VIII and *S. fluitans* III were collected during several research cruises shown in Fig. 1: cruise 64PE455 on the RV *Pelagia* during July-August 2019, where samples were taken from the Central Atlantic and Martinique. The CEMIE-I cruise near Cozumel, where samples were taken near the coast of Mexico during April–May 2019. A research cruise related to the Campaña America Central of INAPESCA-Mexico, where samples were taken in the Caribbean Sea during September–October 2018. Finally, samples were collected in waters near the Bill Bags Cape Florida State Recreation Area in August 2019.

During cruise 64PE455, an ultra-clean CTD system (Seabird 9+, WA, USA) was used to measure temperature, chlorophyll a relative fluorescence, and salinity during water depth profiles. Water samples were taken in Niskin bottles deployed along with the CTD system for subsequent nutrient analyses. Seawater was filtered through a 0.2 μm Acrodisc syringe filter and filtrate samples were preserved in 7 mL vials at −20 °C for phosphate (PO_4), nitrate (NO_3) and nitrite (NO_2), and at 4 °C for Silica (Si). Concentrations of PO_4, NO_3+NO_2, NO_2 and Si (in μM) were measured on a TrAAcs 800 autoanalyzer (Bran+Luebbe, WI, USA) following NSOP 9 guidelines (Hydes et al., 2010). Exact coordinates and additional contextual data of the sampling locations are indicated in Table S1 and on the sampling map in Fig. 1.

2.2. Holopelagic Sargassum collection and identification

Sargassum samples during the cruises and fieldwork were collected using a dipnet that was cleaned with 10% (v/v) bleach solution and 70% (v/v) ethanol solution before sampling. Latex gloves were worn and sterilized with 70% (v/v) ethanol prior to handling the dipnet and any *Sargassum* sample. We sampled separate *Sargassum* clumps as replicates

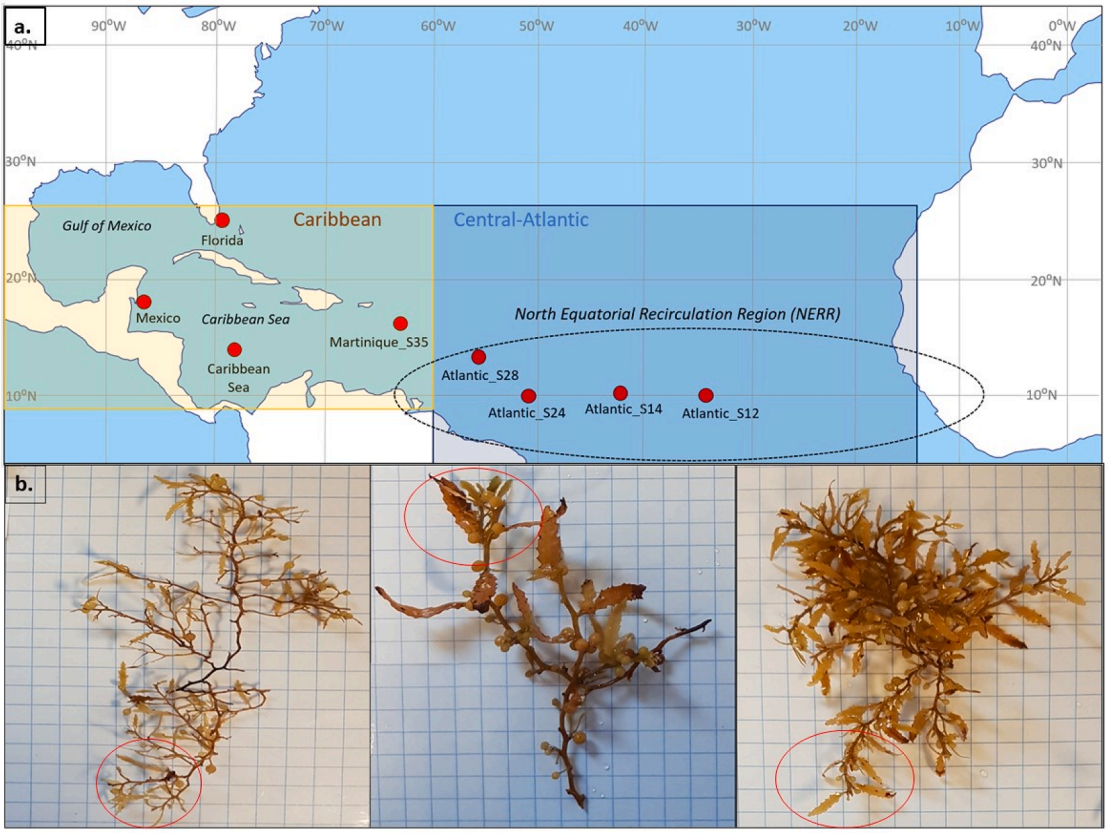

Fig. 1. a. Holopelagic *Sargassum* sampling locations across the Atlantic Ocean and Caribbean and Northern Atlantic coastal regions. Sites are categorized as open ocean, in case of Atlantic stations 12–28, and Caribbean, in case of Mexico, Florida, Caribbean Sea and Martinique_S35. Specific samples per station and coordinates are indicated in Table S1. **b.** Left to right: *Sargassum natans* I, *Sargassum natans* VIII and *Sargassum fluitans* III. Apical tips of the *Sargassum* genotypes were sampled and are indicated with a red ellipse.

($n = 5$) that were minimally 10 m apart in the water and put each clump in a separate bucket that was cleaned with 10% (v/v) bleach solution and 70% (v/v) ethanol solution, then rinsed and filled with 0.2 μm filtered seawater from the station where we collected the *Sargassum*. Each *Sargassum* clump was photographed on 1 cm x 1 cm sterile gridded laminated paper (Fig. 1), and several apical ends of the tissue were removed and placed in silica gel for the microbiome project as described in Quigley et al. (2018). Samples from the same clump were preserved in 70% (v/v) ethanol as a voucher specimen. In total five replicates were taken this way per *Sargassum* genotype, with the exception of the Caribbean Sea location, where between three and five replicates were taken per *Sargassum* genotype summing up to: *S. natans* VIII ($n = 38$), *S. natans* I ($n = 40$) and *S. fluitans* III ($n = 40$) in total. To visualize the microbial biofilm on the macroalgal surface tissue, sub-samples of the *Sargassum* vouchers were prepared for Scanning Electron Microscopy (SEM) analyses from Atlantic stations 12, 24 and 28. SEM samples were dehydrated in an ethanol series as follows: 10 min. in 50%, 70%, 85% and 95%, followed by three times for 10 min. each in 100% (v/v) ethanol. Samples were critical point dried in a Leica CPD300 (Leica Microsystems Inc., Buffalo Grove, IL), sputter coated with 5 nm of platinum using a Leica EM MED020 (Leica Microsystems Inc., Buffalo Grove, IL) and visualized on a Zeiss Supra 40VP SEM (Carl Zeiss Microscopy, Thornwood, NY) at different magnifications as shown in Fig. S1.

We identified holopelagic *Sargassum* genotypes on the basis of morphology as first described in Parr (1939) and consecutive studies (Amaral-Zettler et al., 2017; Schell et al., 2015). *S. fluitans* III is distinguished by the presence of thorns along the stem, *S. natans* I is distinguished by narrow blades and the apical spines on the pneumatocysts and *S. natans* VIII is characterized by large surface blades and a lack of thorns/spines. To confirm genotype assignments we performed a novel molecular genotyping method on shipboard by DNA extraction and subsequent PCR amplification using primers targeting the *Sargassum* mitochondrial genes *cox 2* (*cox2*- 370F: 5′- CAAAGATGGATTCGACGGTTGG- 3′, *cox2*- 776R:5′- CCGGTATCAAACTCGCCCTT- 3′) and *cox3* (467F:5′- GGTTCAACGACACCCATTT- 3′), *cox3*- 901R:5′- TAGCGTGATGAGCCCATG- 3′) as described in Amaral-Zettler et al. (2017). Next, PCR products of *cox2* and *cox3* were cut in enzyme restriction reactions with respective enzymes Eco47III (Thermofisher, MA, USA) and BccI (New England Biolabs, MA, USA) as shown in Fig. S2 following manufacturers' instructions. E-gels (Thermofisher, MA, USA) of 1.2% (w/v) agarose with SYBR Safe DNA Gel Stain (Thermofisher, MA, USA) were run on shipboard during the RV *Pelagia* expedition and in the molecular lab to confirm of the holopelagic *Sargassum* genotypes.

2.3. DNA extraction, PCR amplification & Illumina MiSeq sequencing

Large macrofauna was removed and whole *Sargassum* tissue of the apical ends were extracted to capture both associated endophytic and epiphytic communities. Apical ends were crushed by bead beating using a Vortex Genie 2.0 with bead beating adapter (Scientific Industries, NY, USA) for 20 min at 7000 RPM. Total DNA was extracted using the Quick DNA ZYMO Miniprep kit (ZYMO Research, CA, USA) following manufacturer's instructions for non-soil samples. DNA concentrations and quality were measured with a Qubit Fluorometer 2.0 Fluorometer (Invitrogen, Life Technologies, CA, USA) following the high sensitivity protocol and by NanoDrop Spectrophotometer measurements (ThermoFisher, MA, USA).

16S rRNA gene V4 hypervariable region PCR amplification was done

following the protocol of the Earth Microbiome project (Caporaso et al., 2011) using primers 515F (GTGYCAGCMGCCGCGGTAA) (Parada et al., 2016) and 806RB (GGACTACNVGGGTWTCTAAT) (Apprill et al., 2015). Amplification was performed using Platinum™ SuperFi™ DNA Polymerase (Invitrogen, CA, USA) with the following PCR program: 30 s at 98 °C; 28 cycles of 10 s at 98 °C, 15 s at 50 °C, 30 s at 72 °C; final extension at 72 °C for 5 min and storage at 4 °C. PCR products were quantified by electrophoresis on 2% (w/v) agarose gels for 60 min. at 90 V, staining for 20 min. in ethidium bromide and 10 min. destaining in 1x Tris acetate EDTA (TAE). Samples were amplified in triplicate PCR reactions and pooled after positive gel confirmation. Negative controls (PCR H_2O without template added) and a positive control (*E. coli* gDNA as template) were included in every separate PCR reaction. PCR products from all samples were pooled in equimolar concentrations at 2 ng/μL per sample and ran on a 2% (w/v) agarose gel stained with SYBR green. The 300 bp band, representing the 515F-806RB 16S rRNA gene fragment, was carefully cut out and gel extracted with the Qiaquick Gel Extraction Kit following manufacturer's instructions (Qiagen, Hilden, Germany). Sequencing was performed by the Utrecht Sequencing Facility (Useq, Utrecht, The Netherlands) on an Illumina MiSeq sequencing platform using the Illumina MiSeq 2 × 300bp V3 kit and TruSeq Nano DNA kit (Illumina, CA, USA) following manufacturer's instructions resulting in 19,497,795 reads in total. Raw sequencing data and MIMARKS metadata (Table S3) of this study have been deposited in the European Nucleotide Archive under accession number PRJEB58262.

2.4. Bioinformatic analyses

Amplicon sequencing data were processed with the Cascabel pipeline (Asbun et al., 2020). Processing steps included a quality assessment of the reads with FastQC v0.11.9 (Andrews, 2010), paired read alignment and merging to form a single contig sequence using PEAR v0.9.10 (Zhang et al., 2014), barcode extraction and library demultiplexing using QIIME v1.9.1 and Vsearch v2.8.0 (Caporaso et al., 2010; Rognes et al., 2016) and forward and reverse read concatenation. The combination of forward and reverse reads resulted in 114,217 clean reads on average per sample. DADA2 v1.19.1 (Callahan et al., 2016) identified Amplicon Sequence Variants (ASV) using the following settings: forward and reverse reads were paired with a minimum overlap of 10 nucleotides, sequences were length filtered with a minimum length of 243 bp and maximum length of 262 bp based on a frequency histogram, chimeras were removed, and ASVs were assigned taxonomy using the SILVA SSURef database v138.1. An ASV table was constructed with BIOM v2.1.6 (McDonald et al., 2012). Further filtering of the 16S amplicon data was done in R v4.0.5 (R Core Team, 2013), where ASVs resembling mitochondria and plastids were removed, occurring at ±27% in the dataset on average. Lastly, ASVs occurring 10 times or less in the total dataset were filtered out and read counts were normalized on the basis of the median in Phyloseq v1.34.0 (McMurdie and Holmes, 2013) resulting in 74,675 high-quality reads on average per sample.

To compare our amplicon data with that from Michotey et al. (2020), we downloaded the raw 16S rRNA gene sequence data from Michotey et al. (2020) from the NCBI Sequence Read Archive with accession number PRJNA597297. Data were analyzed with the Cascabel pipeline (Asbun et al., 2019) wherein reads were merged with Vsearch v2.8.0 (Rognes et al., 2016), OTUs were clustered with Uclust v1.9.1 (Edgar, 2010), QIIME 1.9.1 (Caporaso et al., 2010) was implemented to pick representative sequences and taxonomy was assigned with Vsearch v2.8.0. (Rognes et al., 2016). The resulting OTUs and ASVs from our study matching the *Vibrio* genus were selected and imported into ARB v6.0.6 (Ludwig et al., 2004) within the SILVA SSURef database v138.1. We used the "quick add sequence to tree" feature in ARB to add our ASVs and the recalculated OTUs from Michotey et al. (2020) to the reference phylogenetic tree included in the SILVA SSURef database v138.1. The tree was pruned to include only the OTU/ASV sequences matching *Vibrio* and those of *Vibrio* type strains (designated as "s[T]" in ARB) determined using the search and query function of ARB. The pruned phylogenetic tree was further refined with the iTOL interactive tool (Letunic and Bork, 2007) to group ASVs and OTUs that did not cluster with known pathogenic *Vibrio* type strains. *Vibrio* type strains marked as pathogenic were: *V. parahaemolyticus, V. europaeus, V. tubiashii, V. campbelli, V. ichthyoenteri, V. alginolyticus, V. cholerae, V. vulnificus, V. fluvialis, V.aerogenes, V. mimicus, V. harveyi, V. corallillyticus* and *V. rotiferianus* (Austin and Zhang, 2006; Michotey et al., 2020; Osunla and Okoh, 2017; Thompson et al., 2004).

2.5. Statistical analyses

Statistical analyses were performed in R v4.0.5 with the Phyloseq package v1.34.0 (McMurdie and Holmes, 2013) and microbiome package v1.12.0 (Lahti and Sudarshan, 2017). To show the differences in relative microbial abundances at family/genus level, bar graphs were plotted in Microbiome Analyst (Dhariwal et al., 2017). Non-parametric permutational multivariate analysis of variance (PERMANOVA) statistical tests were done (permutations = 9999) to determine statistical differences between the microbiomes of the holopelagic *Sargassum* genotypes and locations with vegan v2.5–7 (Oksanen et al., 2020), after confirming homogeneity of group dispersions using Betadisper.

A Venn diagram was constructed using the R microbiome package v1.12.0 (Lahti and Sudarshan, 2017) and eulerr package 6.1.0 (Larsson, 2021), computing the presence and absence of different ASVs. Shannon diversity indices of samples per *Sargassum* genotype were calculated in Microbiome Analyst and indices did not meet standards for normality nor homoscedasticity according to Shapiro Wilk's test and comparisons of variances in R. A Kruskal-Wallis test was therefore done followed by Mann Whitney U post-hoc tests to reveal pairwise differences between *Sargassum* genotype microbiomes.

Linear discriminant analysis Effect Size (LEfSe) analyses (Segata et al., 2011) were done at the genus level with the Galaxy tool (Goecks et al., 2010) to perform linear discriminant analyses (LDA) to determine holopelagic *Sargassum* genotype/biogeographical specificity and possible biomarkers (Fig. 3& Fig. S4). To plot differences in the community composition on the ASV level of different samples, a non-metric multidimensional scaling plot (NMDS) was constructed using Phyloseq with a stress factor of 0.1207 after 100 runs. The statistical program STAMP (Parks et al., 2014) was used to plot the relative abundances of sequences belonging to the *Vibrio* genus in a box plot. Shapiro Wilk tests and variance comparisons were performed to check for ANOVA assumptions (normality and homoscedasticity). An ANOVA uncovered statistical differences per sampling location for the *Vibrio* genus. A post hoc Tukey HSD test determined statistical differences among holopelagic *Sargassum* genotype and location combinations.

3. Results

3.1. Microbial community characterization of different holopelagic *Sargassum* genotypes

We found that the relative abundance of associated microbial communities at the family level differed among *Sargassum* genotypes (PERMANOVA, $p < 0.001$), though the same predominant families were abundant across them (Fig. 2). First, *Sargassum* microbial communities at the family level showed a large abundance of *Pseudomonadaceae*, constituting from 40% to 60% of the microbial community. *Pseudomonadaceae* was relatively more abundant in *S. natans* VIII (60%) compared to *S. fluitans* III (40%). Other abundant families in the *Sargassum* microbiome were *Rhodobacteraceae* (6–12%), *Vibrionaceae* (3–6%), *Microtrichaceae* (3–5%), *Phormidesmiaceae* (2–4%) and *Nostocaceae* (2–4%) on average. Rare microbial families (<2%) showed higher relative abundance in *Sargassum fluitans* III and included *Saprospiraceae, Ardenticatenales_fam, Cyanobacteriia_ord_fam, Hyphomonadaceae, Caldilineaceae, Endozoicomonadaceae, Pirellulaceae* and *Rhizobiaceae.*

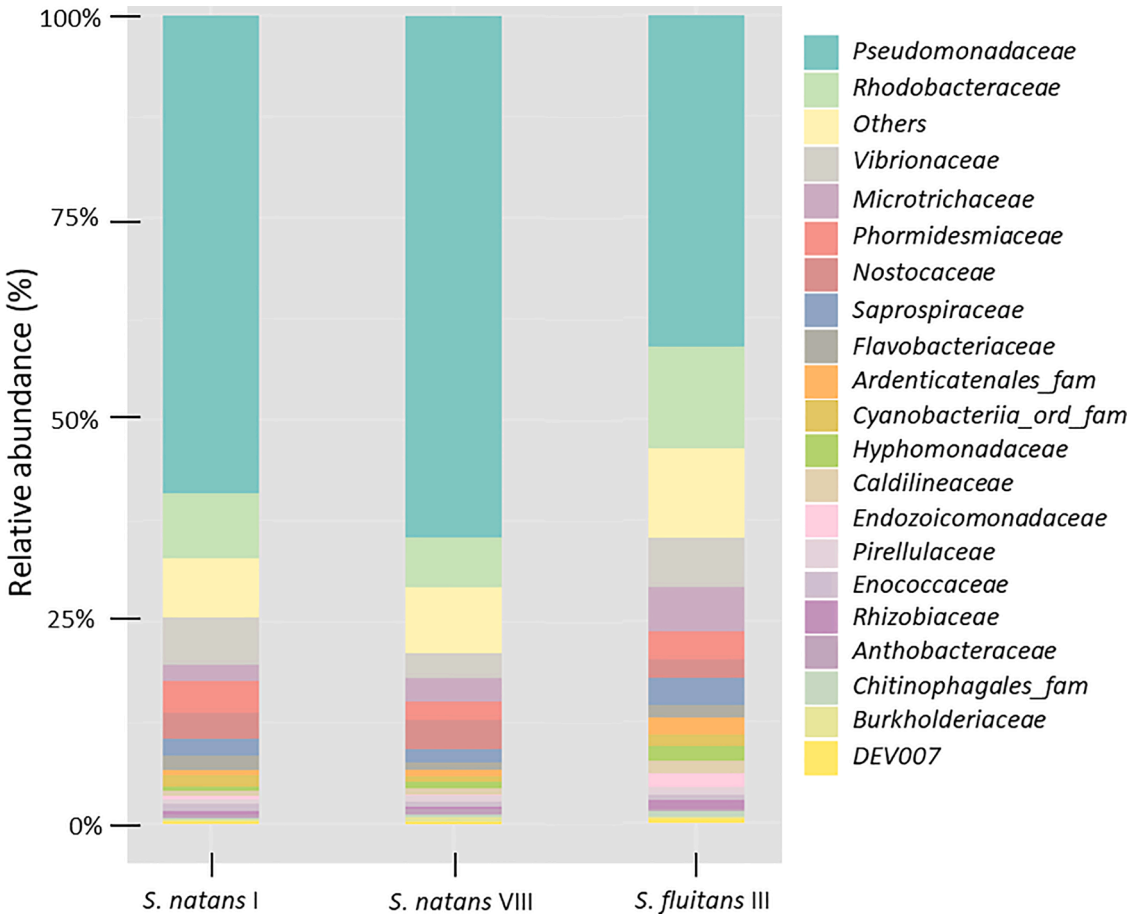

Fig. 2. Average relative abundances (in%) of bacterial taxa at the family level belonging to *Sargassum* genotypes *S. natans* I ($n = 40$), *S. natans* VIII ($n = 38$) and *S. fluitans* III ($n = 40$). The 20 most abundant families are shown, less abundant families are summarized in "Others".

Pseudomonadaceae, Rhodobacteraceae and *Vibrionaceae* summed together contributed 55% – 70% in relative abundance in the three *Sargassum* genotypes, dominating the bacterial families found in the *Sargassum* microbiome.

LEfSe analyses highlighted 20 genera with an LDA score higher than 4.0, that varied strongly between *Sargassum* genotypes and could

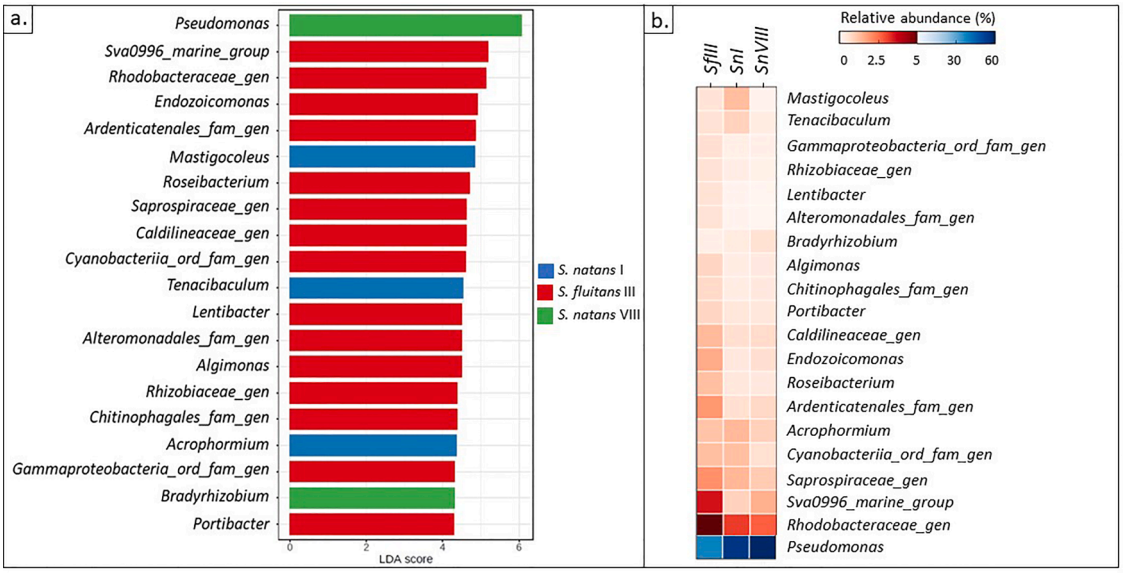

Fig. 3. a. Linear discriminant analyses (LDA) scores of bacterial genera from LEfSe analyses. Microbial genera are sorted by their LDA score that is displayed on the x-axis. Different colors indicate which *Sargassum* genotype displayed the highest relative abundance of the microbial genus and showed *Sargassum* genotype specificity. **b.** Relative abundances of 20 bacterial genera (in%) analyzed in LEfSe analyses of *S. natans* I, *S. natans* VIII and *S. fluitans* III. Color intensity in red/blue indicates relative abundances and taxa are sorted according to their average abundances in the microbial community.

function as biomarkers (Fig. 3). Most of these genera had the highest relative abundance in the *S. fluitans* III microbiome (15 of 20), and included *Roseibacterium* and genera within *Rhodobacteraceae*, and *Saprospiraceae*. The highest LDA score and the genus that varied the most among *Sargassum* genotypes was *Pseudomonas*, that had the highest relative abundance associated with *S. natans* VIII. Furthermore, *Mastigocoleus, Tenacibaculum* and *Acrophormium* showed high LDA scores and were positive indicators for *S. natans* I.

At the ASV level, a total of 5965 ASVs were identified, of which 2602 ASVs (43%) were shared across the three *Sargassum* genotypes (Fig. 4). Though *Sargassum* genotypes exhibited differences as well, since 889 and 862 ASVs (±14%) were unique for *S. natans* VIII and *S. fluitans* III respectively, and 623 ASVs (10%) were unique for *S. natans* I. *S. natans* I and *S. fluitans* III had the most ASVs in common, making *S. natans* VIII the most unique *Sargassum* genotype on the basis of microbial ASV presence/absence. We detected the largest number of different ASVs and the richest microbial community in *S. fluitans* III, with a total of 4315 ASVs. Shannon's diversity indices of the microbiomes of holopelagic *Sargassum* significantly differed between *Sargassum* genotypes (Kruskal-Wallis, $p = 0.006$). The microbiome of *S. fluitans* III was significantly more diverse on the basis of Shannon's diversity indices compared to *S. natans* I and VIII, with 3.5 on average (Mann-Whitney U test, $p = 0.002$ (*S. fluitans* III – *S. natans* I) and $p = 0.016$ (*S. fluitans* III – *S. natans* VIII)). *S. natans* I and *S. natans* VIII displayed similar levels of diversity basis of Shannon's diversity indices (e.g., around 2.2–2.5 (Fig. 4)). However, there was a large spread among biological replicates for the Shannon's diversity index, as shown in the first quartile (0.8) and third quartile values (4.2) of the box plot of *S. natans* I.

3.2. Microbial community differences based on geographic location

The NMDS plot showed variation among holopelagic *Sargassum* genotype and location and a PERMANOVA statistical test showed significant differences between locations ($p < 0.001$) (Fig. 5). In general, microbial communities varied strongly between biological replicates, as shown by the wide distribution of replicates across the NMDS plot. However, a clear separation was displayed between the microbial communities sampled from Florida waters and two replicates from the Caribbean Sea as opposed to the rest of the locations that clustered together in the NMDS plot, indicating differences in the microbial community composition. *Sargassum* microbial communities from the open Atlantic Ocean, Martinique station 35 and Mexico overlapped in the NMDS plot, indicating similar microbial community compositions. Moreover, a difference in microbial communities per *Sargassum* genotype is shown in the NMDS plot, for instance in microbial communities from Atlantic station 14, where replicates of *S. natans* I, *S. natans* VIII and *S. fluitans* III are separated from each other.

Sampling locations appeared to predominantly differ in their relative abundances of *Vibrio* (Fig. 6). The relative abundances of microbial taxa belonging to *Vibrio* significantly differed between locations (ANOVA, $p < 0.001$). *Vibrio* taxa were in low abundances in the Atlantic Ocean locations (<1%), but increased in the more coastal sites of Atlantic station 35, the Caribbean Sea, Florida and Mexico. *Vibrio* reached high relative abundances in two *Sargassum* replicates taken from the Caribbean Sea (55% and 43%) and significantly higher abundances in samples taken near Florida, with 20–35% average relative abundances (Tukey HSD tests, $p < 0.05$). The data set was also analyzed after removing the Florida and Caribbean samples with very high *Vibrio* values to ensure these outliers did not unduly influence the results for the rest of the samples. PERMANOVA analyses showed that even without these samples there are significant differences between microbiomes of the different forms of *Sargassum*, as well as between locations ($p = 0.002$).

Sequences belonging to the *Vibrio* genus of this study and the study from Michotey et al. (2020) were further placed in a phylogenetic tree. Analysis of the phylogenetic placement of OTUs that we obtained with the sequence dataset of Michotey et al. (2020) and the ASVs from our study showed the presence of 18 potential OTUs/ASVs that clustered with type strains of the pathogenic species *Vibrio vulnificus* (4 OTUs, 3 ASVs), *Vibrio tubiashii* (3 ASVs), *Vibrio ichthyoenteri* (1 ASV), *Vibrio parahaemolyticus* (1 OTU, 1 ASV) and *Vibrio rotiferianus* (5 OTUs) (Fig. 7). Twelve of the 18 potential pathogenic OTUs/ASVs showed a similarity of more than 98% (Table 1).

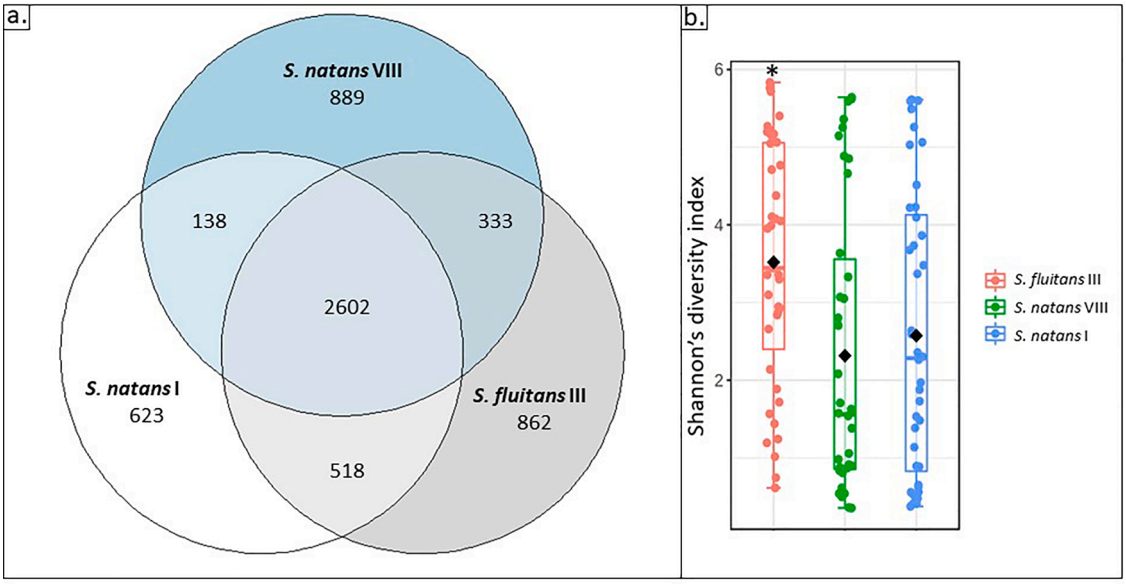

Fig. 4. a. Venn-diagram displaying the total number of amplicon sequence variants (ASVs) either unique for or shared among *Sargassum* genotypes *S. natans* I ($n = 40$), *S. natans* VIII ($n = 38$) and *S. fluitans* III ($n = 40$). A total number of 5965 ASVs are displayed whereby 2602 were shared among all three *Sargassum* genotypes. **b.** Box plot showing Shannon's diversity indices of the microbial communities belonging to *Sargassum* genotypes *S. natans* I, *S. natans* VIII and *S. fluitans* III. The top of the box indicates the third quartile, the bottom of the box indicates the first quartile. The median is shown by the colored middle line, while the black diamond shows the mean. An asterisk indicates significant differences on the $p < 0.05$ level (Mann-Whitney U tests).

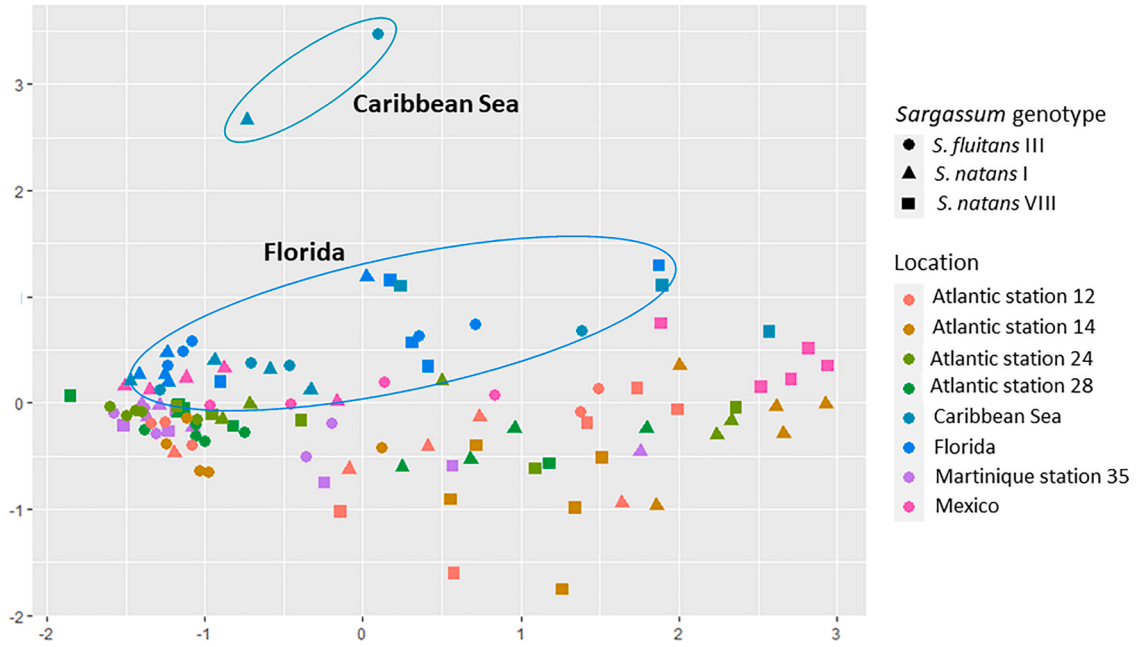

Fig. 5. NMDS plot showing the differences in microbial community beta diversity associated with the *Sargassum* genotypes *S. natans* I ($n = 40$), *S. natans* VIII ($n = 38$) and *S. fluitans* III ($n = 40$) over different locations at the amplicon sequence variant (ASV) level (stress factor = 0.120). The *Sargassum* genotypes are displayed by symbol shape and the location is indicated by color. Two ellipses show the spread of microbial communities belonging to locations of Florida and two locations of the Caribbean Sea.

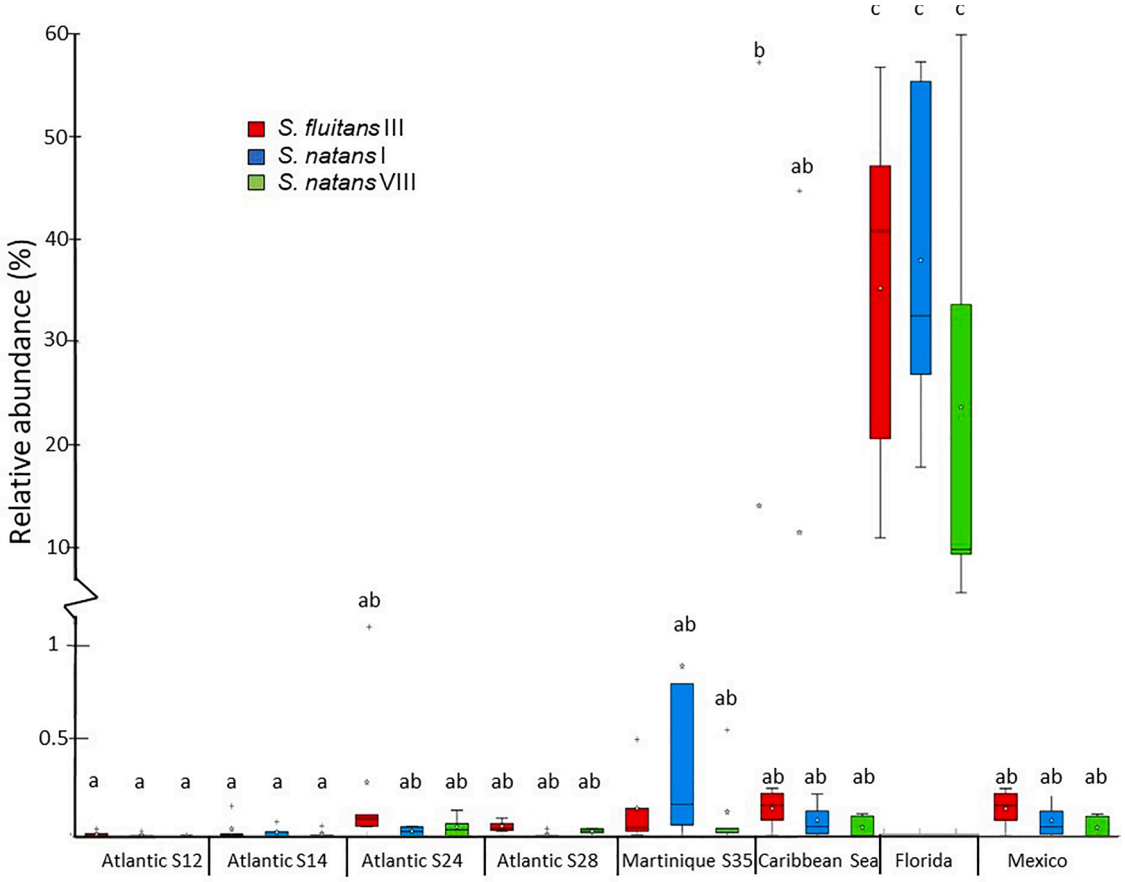

Fig. 6. Box plot showing the relative abundances of amplicon sequence variants (ASVs) belonging to the genus *Vibrio* in the microbial communities of *Sargassum* genotypes *S. natans* I, *S. natans* VIII and *S. fluitans* III ($n \geq 3$). The top of the box indicates the third quartile, the bottom of the box indicates the first quartile. The median is shown by the middle line, while the star shows the mean. Outliers are shown by a plus sign. The letters indicate significant differences at the $p < 0.05$ level (Tukey HSD tests).

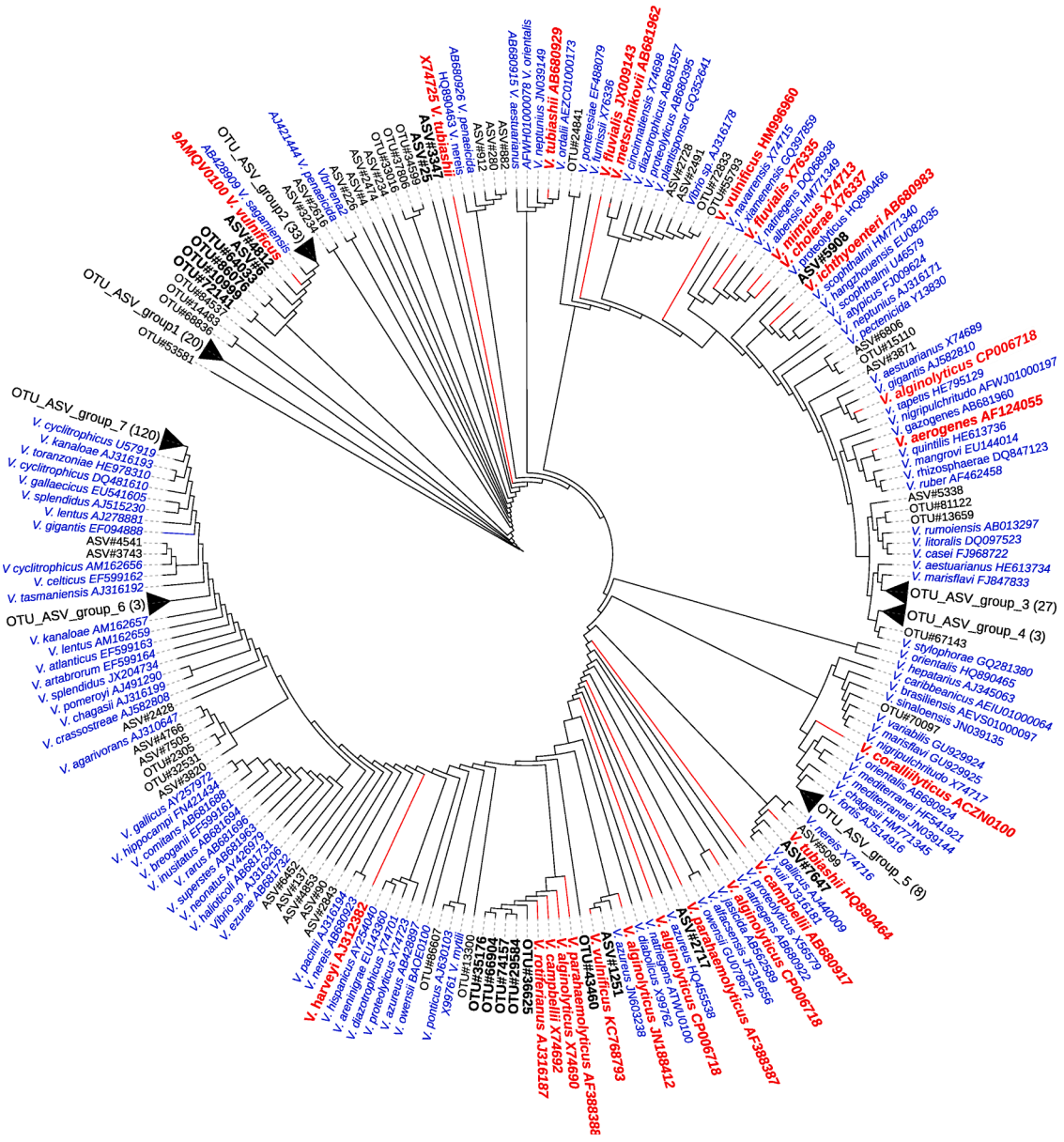

Fig. 7. Phylogenetic tree showing the location of amplicon sequence variants (ASVs) of this study and Operational Taxonomic Units (OTUs) from Michotey et al. (2020) matching *Vibrio*, placed among *Vibrio* type strain representatives of SILVA. Blue indicates *Vibrio* type strains, black indicates ASVs/OTUs, red indicates known *Vibrio* type strain pathogens and bold indicates possible pathogenic OTUs and ASVs.

4. Discussion

We characterized the microbial community of holopelagic *Sargassum* across the GASB and several coastal stranding locations. Specimens of *Sargassum* genotypes *S. natans* I, *S. natans* VIII and *S. fluitans* III were collected across a wide biogeographic distribution from locations spread through the Atlantic Ocean, and several coastal locations in the Caribbean Sea, Florida and Mexico.

4.1. Characterization of holopelagic Sargassum microbial communities

Our results showed that the microbial community compositions of three *Sargassum* genotypes differed significantly from each other, though they contained the same broad microbial families. There was an overwhelming abundance of ASVs belonging to proteobacterial families *Pseudomonadaceae, Rhodobacteraceae* and *Vibrionaceae* present in the holopelagic *Sargassum* microbiome, forming the majority of these microbial communities. This matches well with previous studies on the microbiome of holopelagic *Sargassum* by Michotey et al. (2020), Hervé et al. (2021) and Torralba et al. (2017) that showed that the phylum Proteobacteria or specifically *Alphaproteobacteria* and *Gammaproteobacteria* were among the most abundant classes of bacteria. These observations were also reported for the benthic *Sargassum muticum* (Serebryakova et al., 2018) and *Sargassum ilicifolium* (Oh et al., 2021). The high abundances of *Rhodobacteraceae, Pseudomonadaceae* and *Vibrionaceae* were likely related to the high release of dissolved organic matter (DOM) by holopelagic *Sargassum* in open waters (Powers et al., 2019; Shank et al., 2010a; Shank et al., 2010b), which stimulates the proliferation of DOM-degrading bacteria in these families of *Proteobacteria* (Buchan et al., 2014; Hervé et al., 2021).

Although it is known that the microbiome of both benthic and holopelagic *Sargassum* contain high numbers of *Proteobacteria, Pseudomonadaceae/Pseudomonas* specifically has not been previously shown in such high abundances in holopelagic *Sargassum*. In contrast, Michotey et al. (2020), that studied the surface microbiome after sonification, identified the order *Pseudomonadales* in fairly low abundances of 2–3%

Table 1
Overview of operational taxonomic units (OTUs) and amplicon sequence variants (ASVs) matching pathogenic *Vibrio* in the phylogenetic tree (Fig. 7) sorted by their *Vibrio* match and accession number. Percentage similarity of neighbor joining distance matrices is displayed between OTU/ASVs and *Vibrio* species and rows are highlighted if the similarity percentage is higher than 98%.

Potentially pathogenic *Vibrio* match	OTU and ASV number	Percent similarity (%)
Vibrio vulnificus 9AMQV0100	ASV#6	99.21%
Vibrio vulnificus 9AMQV0100	ASV#4812	99.21%
Vibrio vulnificus 9AMQV0100	OTU#64033	99.2 %
Vibrio vulnificus 9AMQV0100	OTU#86076	99.4%
Vibrio vulnificus 9AMQV0100	OTU#10999	97.43%
Vibrio vulnificus 9AMQV0100	OTU#72141	96.84%
Vibrio vulnificus KC768793	ASV#1251	99.2%
Vibrio tubiashii X74725	ASV#3347	99.6%
Vibrio tubiashii X74725	ASV#25	99.21%
Vibrio tubiashii HQ890464	ASV#7647	96.82%
V. ichthyoenteri AB680983	ASV#5908	98.1%
V. parahaemolyticus AF388387	ASV#2717	99.21%
V. parahaemolyticus AF388388	OTU#43460	99.6%
V. rotiferianus AJ316187	OTU#36625	99.6%
V. rotiferianus AJ316187	OTU#29584	95.65%
V. rotiferianus AJ316187	OTU#74157	95.07%
V. rotiferianus AJ316187	OTU#66904	95.26%
V. rotiferianus AJ316187	OTU#35176	97.33%

on average in the holopelagic *Sargassum* microbiome, as opposed to the averages of 30–50% that were encountered in our study, most notably in *S. natans* VIII. Likewise other marine macroalgal studies targeting species of *Ulva, Splachnidium*, and *Palidina*, also identified *Pseudomonas* species including *P. fluorescens, P. aeruginosa, P. stutzeri, P. pseudoalcaligenes* and *P. putida* (Abdul Malik et al., 2020; Busetti et al., 2017; Califano et al., 2020; Ghaderiardakani et al., 2020). The demonstrated potential of these *Pseudomonas* species in these macroalgae varies between more pathogenic/antimicrobial pathways in the case of pathogens *P. aeruginosa* and *P. stutzeri* (Alhazmi, 2015; Karthick and Mohanraju, 2018), to detoxification of heavy metals in *P. aeruginosa* (De et al., 2008) and utilization of complex carbon sources in *P. pseudoalcaligenes* (Ramya et al., 2017). Both roles as a pathogen and organic matter degrader seem likely in holopelagic *Sargassum*, that produces high concentrations of DOM and hosts a complex interacting micro- and macrofauna community. Further research using cultivation and deep metagenomic sequencing could potentially identify the role of these *Pseudomonas* spp. that are abundant in the microbiome of holopelagic *Sargassum*.

Holopelagic *Sargassum* was enriched in largely photoheterotrophic

or phototrophic bacterial families such as *Rhodobacteraceae, Phormidesmiaceae*, and *Nostocaceae*. This is not surprising, since holopelagic *Sargassum* floats in the marine photic zone and provides an important substrate in open waters for biofilm-producing photosynthetic bacteria. The presence of photosynthetic bacteria agrees with earlier studies on holopelagic *Sargassum* (Hervé et al., 2021; Michotey et al., 2020; Torralba et al., 2017) and these bacteria could assist in nitrogen fixation as has been shown experimentally (Phlips et al., 1986; Phlips and Zeman, 1990). Samples for microbiome comparison in seawater were not analyzed in this study, however *Sargassum* samples were washed with 0.2 μm filtered seawater before processing and it thus likely that the described microbiome is associated with *Sargassum* rather than the neighboring seawater.

4.2. Holopelagic Sargassum genotype-specific microbiomes

Analyses at the genus and ASV level and LEfSe biomarker analyses supported the hypothesis that there are unique bacteria associated with each of the *Sargassum* genotypes. *S. fluitans* III appeared to host the most diverse microbial community and differences were seen among *Sargassum* genotypes through LEfSe biomarker analyses. Interestingly, differences in the associated microbiome among *Sargassum* genotypes were not previously documented, with Michotey et al. (2020) reporting significantly similar microbial communities of holopelagic *Sargassum.* A possible explanation for this may be the methodical differences in sampling of the *Sargassum* microbial communities between studies. In contrast to the whole apical tips that were extracted in our study, Michotey et al. (2020) and Hervé et al. (2021) studied the holopelagic *Sargassum* microbiome on the surface of the whole tissue through sonification and Torralba et al. (2017) worked with whole *Sargassum* tissue cleaned of epibionts. These are important details since the composition of motile macrofauna on holopelagic *Sargassum* has been suggested to vary per *Sargassum* genotype (Martin et al., 2021) and also been shown to differ for sessile hydroids in particular (Govindarajan et al., 2019) that in turn all may host their own microbiome. Moreover, microbial communities of brown macroalgae can depend highly on the specific algal tissue that is sampled, as shown in *S. muticum* and *Fucus vesiculosus* (Capistrant-Fossa et al., 2021; Serebryakova et al., 2018). It is further likely that differences in morphology between *Sargassum* genotypes, which increases the complexity of niches available for the microbial community (Amaral-Zettler et al., 2017; Rosado-Espinosa et al., 2020; Schell et al., 2015), influence the microbial communities. Lastly, holopelagic *Sargassum* releases an array of different forms of DOC, polyphenols, and carbonate in the environment (Powers et al., 2019; Salter et al., 2020), which might vary between *Sargassum* genotypes, as well differing in their biochemical compositions (Davis et al., 2021; Rodríguez-Martínez et al., 2020). All of these differences between the genotypes of holopelagic *Sargassum* collectively might help to diversify their microbial communities.

4.3. Biogeographic patterning in the holopelagic Sargassum microbiome

Our results specifically show that the holopelagic *Sargassum* microbiome differs over their biogeographical range, particularly as the *Sargassum* accumulations approach shore where they show increasing relative abundances of *Vibrio* ASVs. The ecology of *Vibrio* bacteria is quite versatile, with roles in light emitting symbioses, facultative fermentation and nutrient acquisition (Thompson et al., 2004). Most notably however, some *Vibrio* spp. can have pathogen lifestyles, causing diseases not only in humans (Reidl and Klose, 2002), but also marine organisms like corals (Rosenberg et al., 2009), shrimp (Austin and Zhang, 2006), bivalves (Destoumieux-Garzón et al., 2020) and macroalgae (Ward et al., 2020). These infections may be becoming more common due to elevated sea surface water temperatures in recent years (Rosenberg and Ben-Haim, 2002; Thompson et al., 2004). We found *Vibrio* in higher abundances associated with holopelagic *Sargassum* in near-shore sites which is supported by Hervé et al. (2021) that also found *Vibrionaceae* in highest abundances in coastal sites, suggesting that increases in *Sargassum* might result in increasing risks to coastal populations including seagrass meadows and corals reefs.

Previously, Torralba et al. (2017) analyzed holopelagic *Sargassum* microbiomes in the Gulf of Mexico but did not report the presence of *Vibrio* at all. A reason for this could be that the holopelagic *Sargassum* microbiome presents a degree of seasonality, and the composition of *Sargassum* accumulations differ over each year according to seasonal differences like temperature fluctuations, which has been shown in previous studies in benthic *Sargassum* (Serebryakova et al., 2018). Michotey et al. (2020) did encounter high contributions of *Vibrio*, with relative abundances in holopelagic *Sargassum* microbiomes reaching up to 40% in several locations. However, they hypothesized that *Vibrio* is likely less abundant in coastal sites, since the physiological *Sargassum* state is likely not suitable for *Vibrio* development in these coastal stranding sites, whereas in Hervé et al. (2021) and our study, we show the opposite. The reason for these differences, is likely that the samples analyzed by Michotey et al., 2020 came mainly from open ocean environments.

Comparison of our results with Michotey et al. (2020) showed differences in the presence of different pathogenic *Vibrio* species, such as *V. rotiferianus* that were found only in the Michotey et al. (2020) study but not in ours. Because we re-analyzed the data from Michotey et al. (2020), the observed differences might be due to our respective bioinformatic analysis, such as differences in trimming of the raw sequence reads, use of rarefaction, etc. However, most importantly, the analysis also showed several similarities in the presence of pathogenic species, such as the presence of *V. vulnificus* and *V. parahaemolyticus* indicating that these species might be affiliated with holopelagic *Sargassum*, although further research is needed to confirm this observation.

Several hypotheses could explain the high abundances of *Vibrio* spp. in the coastal locations near Mexico and Florida. First, natural vibrios are more abundant in the surface waters of these coastal locations so holopelagic *Sargassum* could enhance the local *Vibrio* bacteria that occur along the coast of Florida and Mexico. Florida has had frequent reports in recent years of emerging *Vibrio* along the coast causing coral diseases among others, likely related to sewage and runoff pollution and increasing temperatures (Buck, 1990; Conrad and Harwood, 2022; Fang et al., 2019; Jenkins et al., 2021; Ushijima et al., 2020). However, we also saw *Vibrio* associated with holopelagic *Sargassum* in low abundances (<1%) in open ocean locations from Atlantic stations 12–28. This suggests *Vibrio* spp. are typically associated to holopelagic *Sargassum*. Another hypothesis is that when holopelagic *Sargassum* enters coastal waters, there are drastic changes in the macroalgal microbiome (Minich et al., 2018). There have been many reports of discoloration and decay of holopelagic *Sargassum* (van Tussenbroek et al., 2017), when it accumulates in close proximity to the shore (Louime et al., 2017; Resiere et al., 2018; Rodríguez-Martínez et al., 2019). Holopelagic *Sargassum* experiences physiological stress in these accumulative coastal masses, resulting in dysbiosis in the microbiome and potentially increasing relative abundances of *Vibrio*. Further research could focus on the effects of coastal decay on the holopelagic *Sargassum* microbiome and what specific bacteria might be increasing under these conditions, which is of interest to the biological conservation of these coastal stranding areas.

5. Conclusions

The microbiome of holopelagic *Sargassum* contains a diverse microbial community that is mainly composed of phototrophs, organic matter degraders (DOM) and potentially pathogenic bacterial genera. *Sargassum* genotypes contain similar microbial groups at the family level but show specificity at the genus level and contain *Sargassum* genotype-specific ASVs. The holopelagic *Sargassum* microbiome shows biogeographic patterning particularly related to large relative abundances of *Vibrio* ASVs. The sometimes dramatic changes in the microbiome as

holopelagic *Sargassum* approaches shore are probably the result of both the resident microbiome experiencing differences in conditions as it accumulates, in combination with colonization by pre-existing coastal bacteria. As the periodic influxes of holopelagic *Sargassum* accumulations continue to deliver massive amounts of biomass and imported microbiomes to coastal areas, there is increased risk of coastal ecosystem impacts. These are not only risks for coastal management that removes *Sargassum* from the shorelines, but also the coral reef, mangroves, and seagrass ecosystems that are already heavily impacted by *Sargassum*. The variation in microbiome with genotype and source region of holopelagic *Sargassum* suggests that these impacts may be influenced not just by how much *Sargassum* strands, but also by what genotype, and its origins.

Declaration of Competing Interest

The authors declare that they have no known competing financial interests or personal relationships that could have appeared to influence the work reported in this paper.

Data Availability

Sequencing data from this study is available at the European Nucleotide Archive under accession number PRJEB58262 and further data is available in the supplementary of this article.

Acknowledgements

We thank the scientific crew, and specially Victor Hugo Martínez and Juan Domingo Izabal Martínez, of the Campaña América Central 2018, as well as Pablo R. Arenas Fuentes and Dr. Ramón I. Rojas González of INAPESCA. We thank Ismael Mariño and the crew and participating scientists of the CEMIE-1 Expedition 2019, and in particular Cecilia Enríquez and Carlos Rodriguez for providing and processing the hydrographic data. The CEMIE-I expedition was financed by CONACYT-SENER-Sustentabilidad Energética project: FSE-2014–06–249795 CEMIE-Océano. We thank the NIOZ-MRF for preparations for the cruise on the RV *Pelagia* and the crew and fellow scientists for their help during the fieldwork carried out during July-August 2019. We thank Judith van Bleijswijk, Maartje Brouwer and Sanne Vreugdenhil for advice with molecular techniques, and Jan van Ooijen for nutrient analyses. This study received Portuguese national funds from FCT - Foundation for Science and Technology through projects UIDB/04326/2020 and LA/P/0101/2020 and through contract CEECINST/00114/2018. This study was supported by a grant from FAPESP (scholarship 2018/17843–4). We thank the National Save the Sea Turtle Foundation-Funded Research and Scholarship awarded under grant /contract AWD/ProjectID (1112150) for the field collection of the Florida samples.

Supplementary materials

Supplementary material associated with this article can be found, in the online version, at doi:10.1016/j.hal.2022.102369.

References

Abdul Malik, S.A., Bedoux, G., Garcia Maldonado, J.Q., Freile-Pelegrín, Y., Robledo, D., Bourgougnon, N., 2020. Defence on surface: macroalgae and their surface-associated microbiome. Adv. Bot. Res. 95, 327–368. https://doi.org/10.1016/bs.abr.2019.11.009.

Alhazmi, A., 2015. *Pseudomonas aeruginosa* – pathogenesis and pathogenic mechanisms. Int. J. Biol. 7, 44–67. https://doi.org/10.5539/ijb.v7n2p44.

Amaral-Zettler, L.A., Dragone, N.B., Schell, J., Slikas, B., Murphy, L.G., Morrall, C.E., Zettler, E.R., 2017. Comparative mitochondrial and chloroplast genomics of a genetically distinct form of *Sargassum* contributing to recent "Golden tides" in the Western Atlantic. Ecol. Evol. 7, 516–525. https://doi.org/10.1002/ece3.2630.

Andrews, S., 2010. FastQC: a quality control tool for high throughput sequence data. https://www.Bioinformatics.babraham.ac.uk/projects/fastqc/. Version 0.11.9.

Apprill, A., Mcnally, S., Parsons, R., Weber, L., 2015. Minor revision to V4 region SSU rRNA 806R gene primer greatly increases detection of SAR11 bacterioplankton. Aquat. Microb. Ecol. 75, 129–137. https://doi.org/10.3354/ame01753.

Asbun, A.A., Besseling, M.A., Balzano, S., van Bleijswijk, J., Witte, H., Villanueva, L., Engelmann, J.C., 2019. Cascabel: a flexible, scalable and easy-to-use amplicon sequence data analysis pipeline. bioRxiv 1–8. https://doi.org/10.1101/809384.

Asbun, A.A., Besseling, M.A., Balzano, S., van Bleijswijk, J.D.L., Witte, H.J., Villanueva, L., Engelmann, J.C., 2020. Cascabel: a scalable and versatile amplicon sequence data analysis pipeline delivering reproducible and documented results. Front. Genet. 11, 1–14. https://doi.org/10.3389/fgene.2020.489357.

Austin, B., Zhang, X.H., 2006. *Vibrio harveyi*: a significant pathogen of marine vertebrates and invertebrates. Lett. Appl. Microbiol. 43, 119–124. https://doi.org/10.1111/j.1472765X.2006.01989.x.

Brooks, M.T., Coles, V.J., Hood, R.R., Gower, J.F.R., 2018. Factors controlling the seasonal distribution of pelagic *Sargassum*. Mar. Ecol. Prog. Ser. 599, 1–18. https://doi.org/10.3354/meps12646.

Buchan, A., LeCleir, G.R., Gulvik, C.A., González, J.M., 2014. Master recyclers: features and functions of bacteria associated with phytoplankton blooms. Nat. Rev. Microbiol. 12, 686–698. https://doi.org/10.1038/nrmicro3326.

Buck, J.D., 1990. Potentially pathogenic marine *Vibrio* species in seawater and marine animals in the Sarasota, Florida, area. J. Coast. Res. 6, 943–948.

Busetti, A., Maggs, C.A., Gilmore, B.F., 2017. Marine macroalgae and their associated microbiomes as a source of antimicrobial chemical diversity. Eur. J. Phycol. 52, 452–465. https://doi.org/10.1080/09670262.2017.1376709.

Butler, J.N., Stoner, A.W., 1984. Pelagic *Sargassum*: has its biomass changed in the last 50 years? Deep Sea Res. Part A. Oceanogr. Res. Pap. 31 (10), 1259–1264.

Califano, G., Kwantes, M., Abreu, M.H., Costa, R., Wichard, T., 2020. Cultivating the macroalgal holobiont: effects of integrated multi-trophic aquaculture on the microbiome of *Ulva rigida* (Chlorophyta). Front. Mar. Sci. 7, 1–19. https://doi.org/10.3389/fmars.2020.00052.

Callahan, B.J., McMurdie, P.J., Rosen, M.J., Han, A.W., Johnson, A.J.A., Holmes, S.P., 2016. DADA2: high-resolution sample inference from illumina amplicon data. Nat. Methods 13, 581–583. https://doi.org/10.1038/nmeth.3869.

Capistrant-Fossa, K.A., Morrison, H.G., Engelen, A.H., Quigley, C.T.C., Morozov, A., Serrão, E.A., Brodie, J., Gachon, C.M.M., Badis, Y., Johnson, L.E., Hoarau, G., Abreu, M.H., Tester, P.A., Stearns, L.A., Brawley, S.H., 2021. The microbiome of the habitat-forming brown alga *Fucus vesiculosus* (Phaeophyceae) has similar cross-Atlantic structure that reflects past and present drivers1. J. Phycol. https://doi.org/10.1111/jpy.13194.

Caporaso, J.G., Kuczynski, J., Stombaugh, J., Bittinger, K., Bushman, F.D., Costello, E.K., Fierer, N., Peña, A.G., Goodrich, J.K., Gordon, J.I., Huttley, G.A., Kelley, S.T., Knights, D., Koenig, J.E., Ley, R.E., Lozupone, C.A., Mcdonald, D., Muegge, B.D., Pirrung, M., Reeder, J., Sevinsky, J.R., Turnbaugh, P.J., Walters, W.A., Widmann, J., Yatsunenko, T., Zaneveld, J., Knight, R., 2010. Correspondence QIIME allows analysis of high- throughput community sequencing data intensity normalization improves color calling in SOLiD sequencing. Nat. Publ. Gr. 7, 335–336. https://doi.org/10.1038/nmeth0510-335.

Caporaso, J.G., Lauber, C.L., Walters, W.A., Berg-Lyons, D., Lozupone, C.A., Turnbaugh, P.J., Fierer, N., Knight, R., 2011. Global patterns of 16S rRNA diversity at a depth of millions of sequences per sample. Proc. Natl. Acad. Sci. U. S. A. 108, 4516–4522. https://doi.org/10.1073/pnas.1000080107.

Conrad, J.W., Harwood, V.J., 2022. Sewage promotes *Vibrio vulnificus* growth and alters gene transcription in *Vibrio vulnificus* CMCP6. Microbiol. Spectr. 10 https://doi.org/10.1128/spectrum.01913-21.

Coston-Clements, L., Settle, L.R., Hoss, D.E., Cross, F.A., 1991. Utilization of the *Sargassum* Habitat by Marine Invertebrates and Vertebrates, A Review (Vol. 296). US Department of Commerce, National Oceanic and Atmospheric Administration, National Marine Fisheries Service, Southeast Fisheries Science Center. US Dep. Commer. Natl. Ocean. Atmos. Adm. Natl. Mar. Fish. Serv. Southeast Fish. Sci. Center, Beaufort Lab, Beaufort, p. 296.

Davis, D., Simister, R., Campbell, S., Marston, M., Bose, S., McQueen-Mason, S.J., Gomez, L.D., Gallimore, W.A., Tonon, T., 2021. Biomass composition of the golden tide pelagic seaweeds *Sargassum fluitans* and *S. natans* (morphotypes I and VIII) to inform valorisation pathways. Sci. Total Environ. 762, 143134 https://doi.org/10.1016/j.scitotenv.2020.143134.

Dawes, C.J., Mathieson, A.C., , The seaweeds of Florida. Univ. Press Florida, De, J., Ramaiah, N., Vardanyan, L., 2008. Detoxification of toxic heavy metals by marine bacteria highly resistant to mercury. Mar. Biotechnol. 10, 471–477. https://doi.org/10.1007/s10126-0089083-z.

De, J., Ramaiah, N., Vardanyan, L., 2008. Detoxification of toxic heavy metals by marine bacteria highly resistant to mercury. Mar. Biotechnol. 10 (4), 471–477.

Destoumieux-Garzón, D., Canesi, L., Oyanedel, D., Travers, M.A., Charrière, G.M., Pruzzo, C., Vezzulli, L., 2020. *Vibrio*–bivalve interactions in health and disease. Environ. Microbiol. 22, 4323–4341. https://doi.org/10.1111/1462-2920.15055.

Devault, D.A., Pierre, R., Marfaing, H., Dolique, F., Lopez, P.J., 2021. *Sargassum* contamination and consequences for downstream uses: a review. J. Appl. Phycol. 33, 567–602. https://doi.org/10.1007/s10811-020-02250-w.

Dhariwal, A., Chong, J., Habib, S., King, I.L., Agellon, L.B., Xia, J., 2017. MicrobiomeAnalyst: a web based tool for comprehensive statistical, visual and meta-analysis of microbiome data. Nucleic Acids Res 45, W180–W188. https://doi.org/10.1093/nar/gkx295.

Djakouré, S., Araujo, M., Hounsou-Gbo, A., Noriega, C., Bourlès, B., 2017. On the potential causes of the recent pelagic *Sargassum* blooms events in the tropical North

Atlantic Ocean. Biogeosciences Discuss 1–20. https://doi.org/10.5194/bg-2017-346.
Edgar, R.C., 2010. Search and clustering orders of magnitude faster than BLAST. Bioinformatics 26, 2460–2461. https://doi.org/10.1093/bioinformatics/btq461.
Fang, L., Ginn, A.M., Harper, J., Kane, A.S., Wright, A.C., 2019. Survey and genetic characterization of *Vibrio cholerae* in Apalachicola Bay, Florida (2012–2014). J. Appl. Microbiol. 126, 1265–1277. https://doi.org/10.1111/jam.14199.
Fidai, Y.A., Dash, J., Tompkins, E.L., Tonon, T., 2020. A systematic review of floating and beach landing records of *Sargassum* beyond the Sargasso Sea. Environ. Res. Commun. 2 https://doi.org/10.1088/2515-7620/abd109.
Fine, M.L., 1970. Faunal variation on pelagic *Sargassum*. Mar. Biol. 7, 112–122.
Ghaderiardakani, F., Quartino, M.L., Wichard, T., 2020. Microbiome-dependent adaptation of seaweeds under environmental stresses: a perspective. Front. Mar. Sci. 7. https://doi.org/10.3389/fmars.2020.575228.
Goecks, J., Nekrutenko, A., Taylor, J., Afgan, E., Ananda, G., Baker, D., Blankenberg, D., Chakrabarty, R., Coraor, N., Goecks, J., Von Kuster, G., Lazarus, R., Li, K., Taylor, J., Vincent, K., 2010. Galaxy: a comprehensive approach for supporting accessible, reproducible, and transparent computational research in the life sciences. Genome Biol. 11 https://doi.org/10.1186/gb-201011-8-r86.
Gouvêa, L.P., Assis, J., Gurgel, C.F.D., Serrão, E.A., Silveira, T.C.L., Santos, R., Duarte, C. M., Peres, L.M.C., Carvalho, V.F., Batista, M., Bastos, E., Sissini, M.N., Horta, P.A., 2020. Golden carbon of *Sargassum* forests revealed as an opportunity for climate change mitigation. Sci. Total Environ. 729, 138745 https://doi.org/10.1016/j.scitotenv.2020.138745.
Govindarajan, A.F., Cooney, L., Whittaker, K., Bloch, D., Burdorf, R.M., Canning, S., Carter, C., Cellan, S.M., Eriksson, F.A.A., Freyer, H., Huston, G., Hutchinson, S., McKeegan, K., Malpani, M., Merkle-Raymond, A., Ouellette, K., Petersen-Rockney, R., Schultz, M., Siuda, A.N.S., 2019. The distribution and mitochondrial genotype of the hydroid *Aglaophenia latecarinata* is correlated with its pelagic *Sargassum* substrate type in the tropical and subtropical western Atlantic Ocean. PeerJ 2019. https://doi.org/10.7717/peerj.7814.
Gower, J., Young, E., King, S., 2013. Satellite images suggest a new *Sargassum* source region in 2011. Remote Sens. Lett. 4, 764–773. https://doi.org/10.1080/2150704X.2013.796433.
Guiry, M.D., Guiry, G.M., 2022. AlgaeBase. World-Wide Electronic Publication. National University of Ireland, Galway. https://www.algaebase.org. searched on 4 February 2022.
Hemphill, A.H., 2005. Conservation on the high seas-drift algae habitat as an open ocean cornerstone. High Seas Mar. Prot. Areas. Park. 15, 48–56.
Hervé, V., Lambourdière, J., René-Trouillefou, M., Devault, D.A., Lopez, P.J., 2021. *Sargassum* differentially shapes the microbiota composition and diversity at coastal tide sites and inland storage sites on Caribbean Islands. Front. Microbiol. 12, 1–14. https://doi.org/10.3389/fmicb.2021.701155.
Hu, C., Wang, M., Lapointe, B.E., Brewton, R.A., Hernandez, F.J., 2021. On the Atlantic pelagic *Sargassum*'s role in carbon fixation and sequestration. Sci. Total Environ. 781, 146801 https://doi.org/10.1016/j.scitotenv.2021.146801.
Hydes, D., Aoyama, M., Aminot, A., Bakker, K., Becker, S., Coverly, S., Daniel, A., Dickson, A.G., Grosso, O., Kerouel, R., van Ooijen, J., Sato, K., Tanhua, T., Woodward, E.M.S., Zhang, J.Z., 2010. Determination of dissolved nutrients (N, P, Si) in seawater with high precision and inter comparability using gas-segmented continuous flow analysers. Go-sh. Repeat Hydrogr. Man. IOCCP Rep. 134, 1–87.
Jenkins, M., Ahmed, S., Barnes, A.N., 2021. A systematic review of waterborne and water-related disease in animal populations of Florida from 1999 to 2019. PLoS ONE 16, 1–21. https://doi.org/10.1371/journal.pone.0255025.
Johns, E.M., Lumpkin, R., Putman, N.F., Smith, R.H., Muller-Karger, F.E.T., Rueda-Roa, D., Hu, C., Wang, M., Brooks, M.T., Gramer, L.J., Werner, F.E., 2020. The establishment of a pelagic *Sargassum* population in the tropical Atlantic: biological consequences of a basin-scale long distance dispersal event. Prog. Oceanogr. 182, 102269 https://doi.org/10.1016/j.pocean.2020.102269.
Johnson, D., Ko, D., Franks, J., 2012. The Sargassum invasion of the Eastern Caribbean and dynamics of the equatorial North Atlantic.
Johnson, D.L., Richardson, P.L., 1977. On the wind-induced sinking of *Sargassum*. J. Exp. Mar. Bio. Ecol. 28, 255–267. https://doi.org/10.1016/0022-0981(77)90095-8.
Karthick, P., Mohanraju, R., 2018. Antimicrobial potential of epiphytic bacteria associated with seaweeds of little Andaman, India. Front. Microbiol. 9, 1–11. https://doi.org/10.3389/fmicb.2018.00611.
Laffoley, D.d'A., Roe, H.S.J., Angel, M.V., Ardon, J., Bates, N.R., Boyd, I.L., Brooke, S., Buck, K.N., Carlson, C.a, Causey, B., Conte, M.H., Christiansen, S., Cleary, J., Donnelly, J., Earle, S.a, Edwards, R., Gjerde, K.M., Giovannoni, S.J., Gulick, S., Gollock, M., Hallett, J., Halpin, P., Hnel, R., Hemphill, A., Johnson, R.J., Knap, a H., Lomas, M.W., McKenna, S.a, Miller, M.J., Miller, P.I., Ming, F.W., Moffitt, R., Nelson, N.B., Parson, L., Peters, A.J., Pitt, J., Rouja, P., Roberts, J., Seigel, D.a, Siuda, a N.S., Steinberg, D.K., Stevenson, A., Sumaila, V.R., Swartz, W., Thorrold, S., Trott, T.M., Vats, V., 2011. The Protection and Management of the Sargasso Sea: The Golden Floating Rainforest of the Atlantic Ocean. Summary Science and Supporting Evidence Case. The golden floating rainforest of the Atlantic Ocean, Sargasso Sea Alliance.
Lahti, L., Sudarshan, S., 2017. Introduction to the microbiome R package. http://microbiome.github.com/microbiome.
Lapointe, B.E., Brewton, R.A., Herren, L.W., Wang, M., Hu, C., McGillicuddy, D.J., Lindell, S., Hernandez, F.J., Morton, P.L., 2021. Nutrient content and stoichiometry of pelagic *Sargassum* reflects increasing nitrogen availability in the Atlantic Basin. Nat. Commun. 12, 1–10. https://doi.org/10.1038/s41467-021-23135-7.
Larsson, J., 2021. eulerr: Area-Proportional Euler and Venn Diagrams With Ellipses. R Packag. Version 6.1.1.
Letunic, I., Bork, P., 2007. Interactive Tree Of Life (iTOL): an online tool for phylogenetic tree display and annotation. Bioinformatics 23 (1), 127–128.
Louime, C., Fortune, J., Gervais, G., 2017. *Sargassum* invasion of coastal environments: a growing concern. Am. J. Environ. Sci. 13, 58–64. https://doi.org/10.3844/ajessp.2017.58.64.
Ludwig, W., Strunk, O., Westram, R., Richter, L., Meier, H., Yadhukumar, A., Buchner, A., Lai, T., Steppi, S., Jacob, G., Förster, W., Brettske, I., Gerber, S., Ginhart, A.W., Gross, O., Grumann, S., Hermann, S., Jost, R., König, A., Liss, T., Lüßbmann, R., May, M., Nonhoff, B., Reichel, B., Strehlow, R., Stamatakis, A., Stuckmann, N., Vilbig, A., Lenke, M., Ludwig, T., Bode, A., Schleifer, K.H., 2004. ARB: a software environment for sequence data. Nucleic Acids Res 32, 1363–1371. https://doi.org/10.1093/nar/gkh293.
Martin, L.M., Taylor, M., Huston, G., Goodwin, D.S., Schell, J.M., Siuda, A.N.S., 2021. Pelagic *Sargassum* morphotypes support different rafting motile epifauna communities. Mar. Biol. 168, 1–17. https://doi.org/10.1007/s00227-021-03910-2.
McDonald, D., Clemente, J.C., Kuczynski, J., Rideout, J.R., Stombaugh, J., Wendel, D., Wilke, A., Huse, S., Hufnagle, J., Meyer, F., Knight, R., Caporaso, J.G., 2012. The biological observation matrix (BIOM) format or: how I learned to stop worrying and love the ome-ome. Gigascience 464, 1–6. https://doi.org/10.1186/2047-217X-1-7.
McMurdie, P.J., Holmes, S., 2013. Phyloseq: an R package for reproducible interactive analysis and graphics of microbiome census data. PLoS ONE 8. https://doi.org/10.1371/journal.pone.0061217.
Michotey, V., Blanfuné, A., Chevalier, C., Garel, M., Diaz, F., Berline, L., Le Grand, L., Armougom, F., Guasco, S., Ruitton, S., Changeux, T., Belloni, B., Blanchot, J., Ménard, F., Thibaut, T., 2020. In situ observations and modelling revealed environmental factors favouring occurrence of *Vibrio* in microbiome of the pelagic *Sargassum* responsible for strandings. Sci. Total Environ. 748, 141216 https://doi.org/10.1016/j.scitotenv.2020.141216.
Minich, J.J., Morris, M.M., Brown, M., Doane, M., Edwards, M.S., Michael, T.P., Dinsdale, E.A., 2018. Elevated temperature drives kelp microbiome dysbiosis, while elevated carbon dioxide induces water microbiome disruption. PLoS ONE 13, 1–23. https://doi.org/10.1371/journal.pone.0192772.
Niermann, U., 1986. Distribution of *Sargassum natans* and some of its epibionts in the Sargasso Sea. Helgol. Meeresuntersuchungen 40, 343–353. https://doi.org/10.1007/BF01983817.
Oh, R.M., Bollati, E., Maithani, P., Huang, D., Wainwright, B.J., 2021. The microbiome of the reef macroalga *Sargassum ilicifolium* in Singapore. Microorganisms 9, 1–11. https://doi.org/10.3390/microorganisms9050898.
Oksanen, J., F. Guillaume Blanchet, Michael Friendly, Roeland Kindt, Pierre Legendre, Dan McGlinn, Peter R. Minchin, R.B. O'Hara, G.L.S., Peter Solymos, M. Henry H. Stevens, E.S. and H.W., 2020. Vegan: community ecology package. R package version 2.5-7. https://CRAN.Rproject.org/package=vegan.
Osunla, C.A., Okoh, A.I., 2017. *Vibrio* pathogens: a public health concern in rural water resources in sub-Saharan Africa. Int. J. Environ. Res. Public Health 14, 1–27. https://doi.org/10.3390/ijerph14101188.
Oviatt, C.A., Huizenga, K., Rogers, C.S., Miller, W.J., 2019. What nutrient sources support anomalous growth and the recent *Sargassum* mass stranding on Caribbean beaches? A review. Mar. Pollut. Bull. 145, 517–525. https://doi.org/10.1016/j.marpolbul.2019.06.049.
Parada, A.E., Needham, D.M., Fuhrman, J.A., 2016. Every base matters: assessing small subunit rRNA primers for marine microbiomes with mock communities, time series and global field samples. Environ. Microbiol. 18, 1403–1414. https://doi.org/10.1111/1462-2920.13023.
Parks, D.H., Tyson, G.W., Hugenholtz, P., Beiko, R.G., 2014. STAMP: statistical analysis of taxonomic and functional profiles. Bioinformatics 30, 3123–3124. https://doi.org/10.1093/bioinformatics/btu494.
Parr, A.E., 1939. Quantitative observations on the pelagic *Sargassum* vegetation of the western north Atlantic. Bull. Bingham Oceanogr. Collect. 6, 1–94.
Partlow, J., & Martinez, G. (2015). Mexico deploys its navy to face its latest threat: monster seaweed. Washington Post, 28. https://www.washingtonpost.com/world/the_americas/mexico-deploysits-navy-to-face-its-latest-threat-monster-seaweed/2015/10/28/cea8ac28-710b-11e5-ba14318f8e87a2fc_story.html.
Phlips, E.J., Willis, M., Verchick, A., 1986. Aspects of nitrogen fixation in *Sargassum* communities off the coast of Florida. J. Exp. Mar. Bio. Ecol. 102, 99–119. https://doi.org/10.1016/00220981(86)90170-X.
Phlips, E., Zeman, C., 1990. Photosynthesis, growth and nitrogen fixation by epiphytic forms of filamentous cyanobacteria from pelagic *Sargassum*. Bull. Mar. Sci 47 (3), 613–621.
Powers, L.C., Hertkorn, N., McDonald, N., Schmitt-Kopplin, P., Del Vecchio, R., Blough, N.V., Gonsior, M., 2019. *Sargassum* sp. act as a large regional source of marine dissolved organic carbon and polyphenols. Global Biogeochem. Cycles 33, 1423–1439. https://doi.org/10.1029/2019GB006225.
Quigley, C.T.C., Morrison, H.G., Mendonça, I.R., Brawley, S.H., 2018. A common garden experiment with *Porphyra umbilicalis* (Rhodophyta) evaluates methods to study spatial differences in the macroalgal microbiome. J. Phycol. 54, 653–664. https://doi.org/10.1111/jpy.12763.
Ramya, R., Devi, S., Manikandan, A., Kannan, V.R., 2017. Standardization of biopolymer production from seaweed associative bacteria. Int. J. Biol. Macromol. 102, 550–564. https://doi.org/10.1016/j.ijbiomac.2017.04.032.
Reidl, J., Klose, K.E., 2002. *Vibrio cholerae* and cholera: out of the water and into the host. FEMS Microbiol. Rev. 26, 125–139. https://doi.org/10.1016/S0168-6445(02)00091-8.
Resiere, D., Mehdaoui, H., Florentin, J., Gueye, P., Lebrun, T., Blateau, A., Viguier, J., Valentino, R., Brouste, Y., Kallel, H., Megarbane, B., Cabie, A., Banydeen, R., Neviere, R., 2020. *Sargassum* seaweed health menace in the Caribbean: clinical characteristics of a population exposed to hydrogen sulfide during the 2018 massive

stranding. Clin. Toxicol. 59, 1–9. https://doi.org/10.1080/15563650.2020.1789162.
Resiere, D., Valentino, R., Nevière, R., Banydeen, R., Gueye, P., Florentin, J., Cabié, A., Lebrun, T., Mégarbane, B., Guerrier, G., Mehdaoui, H., 2018. *Sargassum* seaweed on Caribbean islands: an international public health concern. Lancet 392, 2691. https://doi.org/10.1016/S01406736(18)32777-6.
Rodríguez-Martínez, R.E., Medina-Valmaseda, A.E., Blanchon, P., Monroy-Velázquez, L. V., Almazán-Becerril, A., Delgado-Pech, B., Vásquez-Yeomans, L., Francisco, V., García-Rivas, M.C., 2019. Faunal mortality associated with massive beaching and decomposition of pelagic *Sargassum*. Mar. Pollut. Bull. 146, 201–205. https://doi.org/10.1016/j.marpolbul.2019.06.015.
Rodríguez-Martínez, R.E., Roy, P.D., Torrescano-Valle, N., Cabanillas-Terán, N., Carrillo-Domínguez, S., Collado-Vides, L., García-Sánchez, M., van Tussenbroek, B.I., 2020. Element concentrations in pelagic *Sargassum* along the Mexican Caribbean coast in 2018-2019. PeerJ 8, e8667. https://doi.org/10.7717/peerj.8667.
Rognes, T., Flouri, T., Nichols, B., Quince, C., Mahé, F., 2016. VSEARCH: a versatile open source tool for metagenomics. PeerJ 2016, 1–22. https://doi.org/10.7717/peerj.2584.
Rosado-Espinosa, L.A., Freile-Pelegrín, Y., Hernández-Nuñez, E., Robledo, D., 2020. A comparative study of *Sargassum* species from the Yucatan Peninsula coast: morphological and chemical characterisation. Phycologia 59, 261–271. https://doi.org/10.1080/00318884.2020.1738194.
Rosenberg, E., Ben-Haim, Y., 2002. Microbial diseases of corals and global warming. Environ. Microbiol. 4, 318–326. https://doi.org/10.1046/j.1462-2920.2002.00302.x.
Rosenberg, E., Kushmaro, A., Kramarsky-Winter, E., Banin, E., Yossi, L., 2009. The role of microorganisms in coral bleaching. ISME J 3, 139–146. https://doi.org/10.1038/ismej.2008.104.
Salter, M.A., Rodríguez-Martínez, R.E., Álvarez-Filip, L., Jordán-Dahlgren, E., Perry, C.T., 2020. Pelagic *Sargassum* as an emerging vector of high rate carbonate sediment import to tropical Atlantic coastlines. Glob. Planet. Change 195. https://doi.org/10.1016/j.gloplacha.2020.103332.
Schell, J.M., Goodwin, D.S., Siuda, A.N.S., 2015. Recent *Sargassum* inundation events in the Caribbean: shipboard observations reveal dominance of a previously rare form. Oceanography 28, 8–10. https://doi.org/10.5670/oceanog.2015.70.
Segata, N., Izard, J., Waldron, L., Gevers, D., Miropolsky, L., Garrett, W.S., Huttenhower, C., 2011. Metagenomic biomarker discovery and explanation. Genome Biol 12, R60. https://doi.org/10.1186/gb-2011-12-6-r60.
Serebryakova, A., Aires, T., Viard, F., Serrão, E.A., Engelen, A.H., 2018. Summer shifts of bacterial communities associated with the invasive brown seaweed *Sargassum muticum* are location and tissue dependent. PLoS ONE 13, 1–18. https://doi.org/10.1371/journal.pone.0206734.
Shank, G.C., Lee, R., Vähätalo, A., Zepp, R.G., Bartels, E., 2010a. Production of chromophoric dissolved organic matter from mangrove leaf litter and floating *Sargassum* colonies. Mar. Chem. 119, 172–181. https://doi.org/10.1016/j.marchem.2010.02.002.
Shank, G.C., Zepp, R.G., Vähätalo, A., Lee, R., Bartels, E., 2010b. Photobleaching kinetics of chromophoric dissolved organic matter derived from mangrove leaf litter and floating *Sargassum* colonies. Mar. Chem. 119, 162–171. https://doi.org/10.1016/j.marchem.2010.01.003.
Sissini, M.N., De Barros Barreto, M.B.B., Szećhy, M.T.M., De Lucena, M.B., Oliveira, M.C., Gower, J., Liu, G., De Oliveira Bastos, E., Milstein, D., Gusmão, F., Martinelli-Filho, J.E., Alves-Lima, C., Colepicolo, P., Ameka, G., De Graftjohnson, K., Gouvea, L., Torrano-Silva, B., Nauer, F., Marcos De Castronunes, J., Bonomibarufi, J., Rörig, L., Riosmena-Rodríguez, R., Mello, T.J., Lotufo, L.V.C., Horta, P.A., 2017. The floating *Sargassum* (Phaeophyceae) of the South Atlantic Ocean - likely scenarios. Phycologia 56, 321–328. https://doi.org/10.2216/16-92.1.
Smetacek, V., Zingone, A., 2013. Green and golden seaweed tides on the rise. Nature 504, 84–88. https://doi.org/10.1038/nature12860.
Team, R.C., 2013. R: a language and environment for statistical computing. R found. Stat. Comput. ISBN 3-900051-07-0.
Thompson, F.L., Iida, T., Swings, J., 2004. Biodiversity of Vibrios. Microbiol. Mol. Biol. Rev. 68, 403–431. https://doi.org/10.1128/mmbr.68.3.403-431.2004.
Torralba, M.G., Franks, J.S., Gomez, A., Yooseph, S., Nelson, K.E., Grimes, D.J., 2017. Effect of Macondo prospect 252 oil on microbiota associated with pelagic *Sargassum* in the Northern Gulf of Mexico. Microb. Ecol. 73, 91–100. https://doi.org/10.1007/s00248-016-0857-y.
Ushijima, B., Meyer, J.L., Thompson, S., Pitts, K., Marusich, M.F., Tittl, J., Weatherup, E., Reu, J., Wetzell, R., Aeby, G.S., Häse, C.C., Paul, V.J., 2020. Disease diagnostics and potential coinfections by *Vibrio coralliilyticus* during an ongoing coral disease outbreak in Florida. Front. Microbiol. 11, 1–21. https://doi.org/10.3389/fmicb.2020.569354.
van Tussenbroek, B.I., Hernández Arana, H.A., Rodríguez-Martínez, R.E., Espinoza-Avalos, J., Canizales-Flores, H.M., González-Godoy, C.E., Barba-Santos, M.G., Vega-Zepeda, A., Collado-Vides, L., 2017. Severe impacts of brown tides caused by *Sargassum* spp. on near shore Caribbean seagrass communities. Mar. Pollut. Bull. 122, 272–281. https://doi.org/10.1016/j.marpolbul.2017.06.057.
Wang, M., Hu, C., Barnes, B.B., Mitchum, G., Lapointe, B., Montoya, J.P., 2019. The great Atlantic *Sargassum* belt. Science 365 (6448), 83–87. https://doi.org/10.1126/science.aaw7912.
Ward, G.M., Faisan, J.P., Cottier-Cook, E.J., Gachon, C., Hurtado, A.Q., Lim, P.E., Matoju, I., Msuya, F.E., Bass, D., Brodie, J., 2020. A review of reported seaweed diseases and pests in aquaculture in Asia. J. World Aquac. Soc. 51, 815–828. https://doi.org/10.1111/jwas.12649.
Wells, R.J.D., Rooker, J.R., 2004. Spatial and temporal patterns of habitat use by fishes associated with *Sargassum* mats in the Northwestern Gulf of Mexico. Bull. Mar. Sci. 74, 81–99.
Zhang, J., Kobert, K., Flouri, T., Stamatakis, A., 2014. PEAR: a fast and accurate illumina paired-end reAd mergeR. Bioinformatics 30, 614–620. https://doi.org/10.1093/bioinformatics/btt593.